Available online at www.sciencedirect.com

ScienceDirect

Mendeleev Commun., 2022, **32**, 597–600

Mendeleev Communications

Effect of pressure on the low-temperature reaction of ethylene with N_2O_4

Nikolay N. Tolkachev,*[a] Evguenyi N. Khodot,[a] Iosif I. Lischiner,[b] Olga V. Malova,[b] Vladimir A. Tartakovsky[a] and Valérie Naudet[c]

[a] *N. D. Zelinsky Institute of Organic Chemistry, Russian Academy of Sciences, 119991 Moscow, Russian Federation. E-mail: nick33@ioc.ac.ru*

[b] *Joint Institute of High Temperatures, Russian Academy of Sciences, 125412 Moscow, Russian Federation*

[c] *Air Liquide, Campus Innovation Paris, Les Loges-en-Josas, 78354 JOUY-EN JOSAS, France*

DOI: 10.1016/j.mencom.2022.09.009

Calorimetric monitoring of the autoclave reaction N_2O_4 + C_2H_4 at –85 to +10 °C under argon pressure 10–30 bar revealed that the exothermic chemical reaction started at temperatures above –52 °C at 10 bar, whereas an intensive exothermic reaction started at –85 °C and pressure of 30 bar. IR study showed that oligo/polynitroethylene was formed at 30 bar, while carbonyl and hydroxy compound as well as nitrate R–ONO_2 formation occurred upon processing at 10 bar.

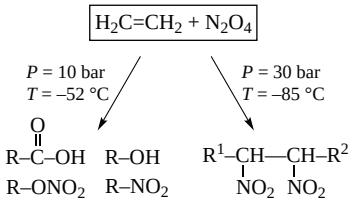

Keywords: ethylene, nitrogen tetroxide, low temperature reactions, ambient heating, pressure effect, nitro compounds.

Different types of unsaturated hydrocarbons as well as of nitrogen oxides can be found as impurities[1,2] in the petrochemical industry and refinery feeds. The reaction of nitrogen oxides with unsaturated hydrocarbons can lead to polymeric nitro compounds (so called 'nitro-gums') which deposit on reactor or pipe walls.[3] This phenomenon is observed by syngas or hydrogen producers at the stage of the cryogenic hydrogen purification. The danger of explosive gum formation due to the reaction of NO_x with conjugated diolefins under cryogenic conditions has been recognized, while formation of nitro-gum is sometimes considered only as a secondary factor in the formation of explosion-hazardous substances when nitro-gums act as solvents for light molecules or labile nitro compounds with oxygen balance close to zero or above it.[4,5]

The addition reactions of nitrogen oxides to unsaturated hydrocarbons have been intensively studied since the beginning of the last century (see review[6]). Certain unsaturated compounds underwent a rapid addition reaction with the mechanism similar to that of free radical reactions.[7–9] These reactions were sensitive to heat transfer properties of the reactor environment. For example, start of the fast reaction can be shifted toward higher temperatures by increase in heat transfer/heat capacity of the reactor environment.[8] Radical nitration is widely used to produce nitroalkanes and nitroalkenes, with nitric acid or nitrogen oxides serving as nitrating agents.

Even though the oxidation chemistry of ethylene has been studied extensively in the past, reports on the behavior at high pressure are sparse. In particular, there is little knowledge about the interaction of ethylene with nitrogen oxides at elevated pressure.[10] It was noticed[11] that the reaction rate of nitrogen oxide with monoolefins, lower dienes and acetylene was very slow and reactions did not start below 0 °C. However, Mikhaylovskaya[12] reported on high reactivity of NO_2 towards ethylene at room temperature and elevated pressures of 10.5 bar (under atmospheric pressure, no conversion was observed even after 70 h).

Nitration reactions are characterized by an induction time of 10–20 min, during which the reaction proceeds very slowly. The induction period can be significantly reduced on heating to 100–350 °C. The mixture with reagents C_2H_4/NO_2 ratio of 2.6 spontaneously warms up within 15 min at P_{ini} = 60 bar and self-ignites then. The color of the liquid products varies from yellow to red-brown. The liquid products contain dissolved or attached nitric oxide that can easily be separated under vacuum. The elemental analysis has shown that the liquid products contained a substantial amount of bound oxygen and nitrogen formed at moderate initial pressures. Under P_{ini} = 15–40 bar, the liquid product had average formula $C_{1.2}H_{3.5}NO_{2.2}$, molecular weight was about 150 Da.[12] The composition of the liquid products formed under P_{ini} = 6 bar was close to $(CH_2)_n$ with a small amount of nitrogen. Under P_{ini} = 60 bar the reaction led to liquid products corresponding to formula C_3H_5NO with high acidity, easily soluble in aqueous alkali solutions, ethyl alcohol, chloroform or tetrachloromethane.

Last publications on the reactions between NO_x and unsaturated hydrocarbons relate mainly to NO_x selective catalytic reduction (NO_x SCR) as well as to studying impact of nitrogen oxide impurities on fuel combustion,[13] which is quite far from the subject of the present article. Typically, the reactions were studied at ambient or slightly elevated pressure. Sometimes nitrogen oxides were used as a source of oxygen atoms for radical processes[14,15] or as a model oxidizing agent.[16] Another modern trend is a study of $^{\bullet}NO_3$ radical reaction with bio- and anthropogenically produced volatile hydrocarbons under conditions of the troposphere.[17] Some studies have been aimed to reveal the effect of $^{\bullet}NO_3$ radical on unsaturated hydrocarbons under ambient air impurities and climate conditions. Those results were used to optimize

industrial processes and to develop adequate detailed kinetic models.[18,19]

The purpose of this work was to study impact of pressure (P = 10–30 bar) on the reaction between C_2H_4 and N_2O_4 under conditions typical for an ambient heating regime of low temperature gas purification units (from –85 to +10 °C). The conditions were selected as typical for industrial equipment operations. Experiments were carried out at a purpose-built laboratory setup consisting of a 75 ml batch reactor unit (autoclave) equipped with control system fitted with temperature and pressure sensors (for the setup appearance and flow diagram, see Online Supplementary Materials, Figure S1). The autoclave is made from stainless-steel XH65MB equipped with a Teflon insert to minimize the influence of the wall material on the reaction. Dichloromethane was used as a solvent for the liquid and solid products since it is inert enough toward both acids and alkalis, and most (>9%) of the reaction products are soluble in it. Dissolved products were analyzed by IR spectroscopy.

Measured time dependences of the temperature inside the reactor look typical for the ambient heating mode (Figure 1). In general, ambient heating occurs according to the Newton's law of cooling. Despite numerous attempts to develop an alternative law (see, *e.g.*, recent ref. 20), the Newton's law of cooling remains the most common way to describe situation when a body is heating or cooling by heat exchange with environment (ambient cooling or heating). The heating rate decreases over time as the driving force for heat transfer decreases (the temperature in the reactor approaches ambient temperature).

To distinguish heat effects of chemical reactions and physical transformations from the temperature changes caused by an ambient heating mode of the operation, the following technique is used. All the measured time dependences of the temperature can be fitted by a straight line in axes ln(ΔT)–time. These axes correspond to the Newton's law of cooling (see Figure 1). Blank experiments of the ambient heating of the reactor filled only with argon were carried out to estimate an impact of possible unaccounted phenomena on the time dependences of the reactor temperature (see Online Supplementary Materials, Figure S2). In the blank experiment some deviations (dashed line in Figure S2) correspond to either temperature changes in heat transfer coefficients or changes in the surrounding conditions (for example, undesirable changes in the convection regime or some water condensation on the reactor walls). Noteworthy, the general shapes of time dependences on temperature for different composition mixtures measured under different pressures are close.

Parameters of the fitting straight lines were found using the least squares method (in the Newton plot). These parameters were used to simulate ambient heating baselines (in axes temperature–time). Found baselines were subtracted from measured temperature dependences. The correlation coefficients

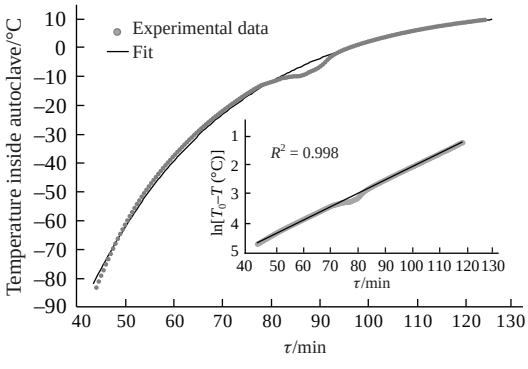

Figure 1 An example of the calorimetric raw data and found fit. Inset: linear approximation in the Newton plot. Mixture of 1.6 mmol N_2O_4 pressured by 30 bar of argon.

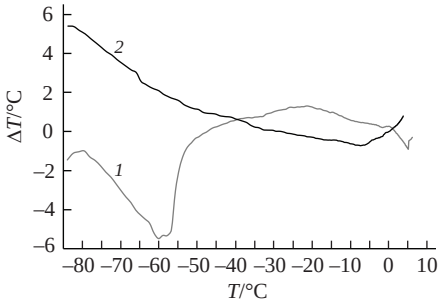

Figure 2 Temperature variations of N_2O_4 + C_2H_4 + Ar mixtures, Ar curve is the reference; (*1*) at 10 bar, (*2*) at 30 bar. (Plot before Ar curve subtraction can be found in Figure S4 of Online Supplementary Materials).

are >0.995 for any found linear trendlines. Points corresponding to temperatures below +5 °C have been taken into account since above +5 °C apparent deviation from linearity was observed. The found coefficients were not analyzed here, since they include many unpredictable parameters affecting experimental data, but they were only used to find a baseline for the measured temperature dependences (see Figure 1). Results of the baseline (fit curve) substruction are presented in Figures S2–S4. Temperature values of the horizontal axis in all the Figures are temperature of the baselines.

Since the reactor was sealed before ambient heating procedure, it is possible to calculate a total amount of gaseous components using ideal gas law [equation (1)] taking the actual pressure and temperature inside the reactor as the input.

$$\Delta N = N_0 - PVR^{-1}T^{-1}, \quad (1)$$

where ΔN is variation of the amount of the reactor gas phase, N_0 is initial amount calculated for conditions just after reactor being pressurized with argon before ambient heating started, T is temperature in the reactor, P is pressure in the reactor, V is free volume of the reactor; R is the gas constant (8.314 J K^{-1} mol^{-1}).

Variations of the amount of substance in the reactor gas phase found by equation (1) are presented in Figures 3, S5 and S6. Figure 4 shows the results of subtraction of the deviation of the

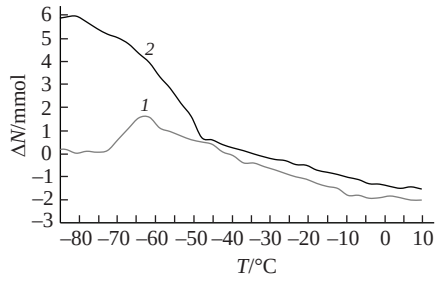

Figure 3 Differential variations of the gas phase substance amount N_2O_4 + C_2H_4 + Ar, C_2H_4 + Ar is the reference; (*1*) at 10 bar, (*2*) at 30 bar.

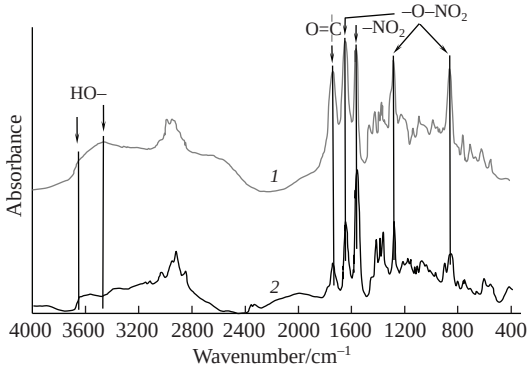

Figure 4 IR spectra of the dichloromethane extract of products from the reaction C_2H_4 + N_2O_4. Reaction pressure: (*1*) 10 bar, (*2*) 30 bar.

amount of the substance found for the mixture of C_2H_4 + Ar from the deviation of the amount of the substance found for the mixture of C_2H_4 + N_2O_4 + Ar. This lets us clearly show the impact of N_2O_4 on the variation of the amount of the substance in the reactor gas phase.

Temperature variations found for N_2O_4 + Ar mixtures in general follow dependence found for Ar only (see Figure S2). The main differences are sharp negative peaks in –15 to –2 °C region. Maximum amplitudes of the negative peaks are dT = –2 °C for 10 bar and dT = –3.5 °C for 30 bar. Negative temperature deviation corresponds to an endothermic process. The observed sharp negative peaks can be attributed to N_2O_4 melting (melting point of N_2O_4 is –11.5 °C[21]). Dependences of temperature variation of the mixtures C_2H_4 + Ar demonstrated the presence of an endothermic process in the very beginning of the heating (at –85 °C and above, see Figure S2). Remarkably that at 30 bar the endothermic effect is much more pronounced than at 10 bar. Negative deviation from the blank Ar curve can be found up to the –60 °C temperature. Mentioned endothermic processes can be rationally attributed to the evaporation of partially condensed ethylene. Positive deviations from the blank curve can be found in the region –60 to –30 °C with maxima locating at –56 °C (10 bar) and –44 °C (30 bar). The origin of these exothermic processes is not clear at the moment (Figure S3).

Temperature deviation curves obtained for mixture N_2O_4, C_2H_4, and Ar at pressures 10 and 30 bar differ seriously. An intensive (dT = –4.5 °C) negative peak at –85 to –60 °C was found for ambient heating at 10 bar (see Figures 3 and S3). It would be logical to attribute the found negative endothermic peak to the evaporation of partially condensed ethylene, but the corresponding peak found in the experiment without N_2O_4 is much less pronounced (dT = –2 °C in comparison with Ar, see Figure S3). As a result, endothermic reaction at 10 bar in the –85 to –60 °C region can be suspected. On the contrary, very intensive (dT > +5 °C) and wide exothermic area was found at 30 bar in the region –85 to –32 °C. It should be outlined that the reaction starts even at lower temperatures. A much less intensive endothermic peak with minimum around –7 °C was found (dT = –0.7 °C, see Figure 2). It can be concluded that increase in pressure from 10 up to 30 bar leads to principal changes in the reaction progress, *viz.*, at 10 bar an endothermic process is followed by an exothermic one while at 30 bar an exothermic process is followed by an endothermic one. Remarkably, pronounced peaks corresponding to N_2O_4 melting are not found if C_2H_4 is present in the mixtures. This fact can be an evidence that N_2O_4 reacts almost completely at temperatures below –15 °C.

Amounts of the gas phase substances were found using ideal gas law on the basis of the temperature and pressure inside the reactor measured directly without any transformations. Comparison of the data in Figures S5 and S6 reveals the similar behavior of the curves corresponding to the mixture of N_2O_4 and argon obtained for the experiments at pressures 10 and 30 bar, whereas for mixtures containing C_2H_4 the picture is principally different. Indeed, if the reactor temperature grows at 10 bar, then the temperature rise from –85 to –60 °C leads to an increase in the amount of a gas phase (Figure S5). Hence, the C_2H_4 evaporation process can be suspected. Another evidence of the ethylene evaporation can be a negative temperature variation obtained for the mixture of N_2O_4, C_2H_4, and argon (see Figure 2). These results bring about some contradictions obtained for the mixture of C_2H_4 and argon since no apparent negative temperature variation was found at 10 bar. This contradiction is not clear now. On the contrary, a jump in the gas phase amount happening somewhere below –85 °C was found. The gas phase amount jump is followed by a smooth decrease during a temperature increase from –85 to –60 °C under 30 bar (Figure S6), the corresponding temperature effect is apparently exothermic (see Figure 2). Notably, the process at 30 bar gets endothermic regime at temperatures higher –25 °C.

More obvious information on the processes taking place can be found in Figure 3 presenting a differential variation of the amount of the gas phase if the curve corresponding to the mixture of C_2H_4 and argon is used as the reference. It is clear that the injection of N_2O_4 leads to a sharp increase in the gas phase amount at temperatures below –85 °C at 30 bar, whereas there is no change in the gas phase amount at temperatures up to –70 °C at 10 bar. Small maximum of amount variation was found around –62 °C. Remarkably, at temperatures above –37 °C differential curves found for both 10 and 30 bar are almost identical and get negative values which is an evidence of reduction of the substance amount in the gas phase in comparison with the initial state of the system. Hence, polymerization or condensation processes can be suspected.

All the products including nitrogen-containing ones were liquid and/or soft wax, no light gas products were found condensed in the cooled trap (–40 °C). IR spectra (see Figure 4) of the liquid products have shown the presence of several functional groups in the reaction products being as follows.[22] (1) Oxidation products: wide absorption band of OH groups at 3600–3300 cm^{-1} and carbonyl groups at 1720 cm^{-1}, (2) products of polymerization/oligomerization: asymmetric stretching vibrations of CH_2 and CH_3 groups at 3000–2850 cm^{-1}, and (3) nitrates R–O–NO_2: 1670, 1280, 835 cm^{-1}, nitro compounds R–NO_2: 1560 cm^{-1}. Analysis of the most intensive adsorption bands allows one to conclude that an increase in pressure suppresses the formation of oxygen-containing compounds, and the most favorable products are organic nitrates.

Thus, proposed analysis of calorimetric data consisting in subtraction of the ambient heating temperature baseline and in combination with analysis of the changes in the amount of gaseous substances and IR spectroscopy allows us to reveal an impact of the pressure on the reaction outcome betwenn N_2O_4 and C_2H_4 at low temperatures. At 30 bar, the reaction starts below –85 °C and is accompanied by a heat evolution, whereas at 10 bar ethylene evaporation is observed and a chemical exothermic reaction can be suspected above –52 °C. As a result, an increase in the pressure lowers the temperature of the reaction start for more than 30 °C (from –52 to below –85 °C). Analysis of IR spectra of the formed products allows one to conclude that lower pressure is favorable for the formation of oxygenates (alcohols, aldehydes, ketones, organic acids) and nitrates (R–O–NO_2), whereas the formation of nitro compounds (R–NO_2) prevails at elevated pressures (30 bar and above). As a result, the reaction scheme can be proposed (Scheme 1). The obtained results provide new information on the mechanism of reaction between nitrogen oxides and olefins and they can be useful for safer designing the low-temperature gas purification systems of petrochemical and waste incineration plants.

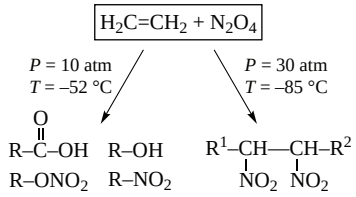

Scheme 1

The manuscript was written through contributions of all authors. All authors have given approval to the final version of the manuscript. All authors contributed equally.

The authors thank physicist Dr. Vladimir V. Frolov for raw data processing and bright ideas he shared.

Online Supplementary Materials

Supplementary data associated with this article can be found in the online version at doi: 10.1016/j.mencom.2022.09.009.

References

1 C. Higman and M. van der Burgt, *Gasification*, Elsevier/Gulf Professional Publishing, 2003.
2 Q. Zhu, X. Zhao and Y. Deng, *J. Nat. Gas Chem.*, 2004, **13**, 191.
3 V. I. Fainshtein, *Kislorod, azot, argon – bezopasnost pri proizvodstve i primenenii* (*Oxygen, Nitrogen, Argon – Safe Production and Use*), Intermed Engineering, Moscow, 2008, p. 21 (in Russian).
4 M. Schnobel, *12AIChE – 2012 AIChE Spring Meeting and 8th Global Congress on Process Safety*, Houston, 2012, p. 16.
5 W. Hack, R. Copeland and D. Hines, *21st AIChE Ethylene Producers Conference*, Tampa, 2009.
6 J. L. Riebsomer, *Chem. Rev.*, 1945, **36**, 157.
7 A. I. Rozlovsky and V. A. Gryaznov, *Dokl. Akad. Nauk SSSR*, 1970, **195**, 133 (in Russian).
8 A. I. Rozlovsky and V. A. Gryaznov, *Dokl. Akad. Nauk SSSR*, 1970, **220**, 1099 (in Russian).
9 V. I. Papisova and G. B. Sergeev, *Dokl. Akad. Nauk SSSR*, 1966, **166**, 1369 (in Russian).
10 J. Giménez-López, M. U. Alzueta, C. T. Rasmussen, P. Marshall and P. Glarborg, *Proc. Combust. Inst.*, 2011, **33**, 449.
11 A. V. Stepanov and V. V. Veselovsky, *Russ. Chem. Rev.*, 2003, **72**, 327 (*Usp. Khim*., 2003, **72**, 363).
12 N. N. Mikhaylovskaya, A. I. Rozlovsky and K. S. Stepanova, *Dokl. Akad. Nauk SSSR*, 1970, **184**, 608 (in Russian).
13 F. Deng, Y. Zhang, W. Sun, W. Huang, Q. Zhao, X. Qin, F. Yang and Z. Huang, *Proc. Combust. Inst.*, 2019, **37**, 719.
14 J. C. Loison, C. Dedonder-Lardeux, C. Jouvet and D. Solgadi, *J. Phys. Chem.*, 1991, **95**, 9192.
15 J. C. Loison, C. Dedonder-Lardeux, C. Jouvet and D. Solgadi, *Faraday Discuss.*, 1994, **97**, 379.
16 J. Liu, W. Zhou, S. D. Chambreau and G. L. Vaghjiani, *J. Phys. Chem. B*, 2020, **124**, 4303.
17 N. L. Ng, S. S. Brown, A. T. Archibald, E. Atlas, R. C. Cohen, J. N. Crowley, D. A. Day, N. M. Donahue, J. L. Fry, H. Fuchs, R. J. Griffin, M. I. Guzman, H. Herrmann, A. Hodzic, Y. Iinuma, J. L. Jimenez, A. Kiendler-Scharr, B. H. Lee, D. J. Luecken, J. Mao, R. McLaren, A. Mutzel, H. D. Osthoff, B. Ouyang, B. Picquet-Varrault, U. Platt, H. O. T. Pye, Y. Rudich, R. H. Schwantes, M. Shiraiwa, J. Stutz, J. A. Thornton, A. Tilgner, B. J. Williams and R. A. Zaveri, *Atmos. Chem. Phys.*, 2017, **17**, 2103.
18 T. L. Nguyen, J. Park, K. Lee, K. Song and J. R. Barker, *J. Phys. Chem. A*, 2011, **115**, 4894.
19 L. Vereecken and J. S. Francisco, *Chem. Soc. Rev.*, 2012, **41**, 6259.
20 H. Sarafian, *Am. J. Comput. Math*., 2021, **11**, 64.
21 P. Gray and A. D. Yoffe, *Chem. Rev.*, 1955, **55**, 1069.
22 E. Pretsch, P. Bühlmann and C. Affolter, *Structure Determination of Organic Compounds: Tables of Spectral Data*, Springer-Verlag, Berlin, Heidelberg, 2000.

Received: 28th March 2022; Com. 22/6841